JOURNAL OF MATERIALS SCIENCE 29 (1994) 1185–1190

'Bundle-debond' technique for characterizing fibre/matrix interfacial adhesion

P. GOPAL, L. R. DHARANI*, N. SUBRAMANIAM‡, FRANK D. BLUM‡
Department of Mechanical and Aerospace Engineering and Engineering Mechanics, and ‡Department of Chemistry, Materials Research Center, University of Missouri-Rolla, Rolla, MO 65401, USA

An experimental technique called bundle-debonding, has been developed for characterizing the interfacial adhesion of fibre bundles and matrix. The specimen is double-notched and contains a partially embedded fibre layer in between the notches. When a tensile load is applied at the specimen ends, the load transfer across the notch and between two pieces of matrix, occurs through the interface between a single layer of fibres and matrix. Kevlar-29 (Kelvar is a registered trademark of E.I. duPont de nemours) fibre tows were used in conjunction with a solid phenolic resin to fabricate the specimens. Experiments were conducted at various embedded lengths resulting in interfacial debond. A simple shear-lag analysis was carried out to determine the interfacial shear strength. The interfacial shear strength of Kevlar-29/phenolic resin has been determined to be 15 MPa. This technique is promising for application on several fibre/matrix systems, specially for fibres of extremely low nominal diameter, supplied as tows.

1. Introduction

A considerable amount of research [1–3] on the interface between the fibre and the matrix in fibre-reinforced composites, has been done during the last three decades. This is because of the key role played by the interfacial bond in determining basic composite properties. Many test methods [4] have been developed and used for the characterization of the fibre/matrix interface. The most notable of the current methods, is the single-fibre pull-out test, wherein a single fibre is pulled out of a matrix button of sufficiently small thickness. Miller *et al.* [5] have argued that the single-fibre pull-out test is limited to embedding reasonably large diameter fibres in a pool of matrix. In order to improve this situation, they have developed the microbond method for characterizing the single-fibre/matrix interface. This method consists of curing a droplet of resin on the single fibre and pulling out the fibre from the droplet. The microbond method involves the replacement of the matrix button with a matrix droplet and requires the use of a liquid resin. With this method, one also has to work with a single fibre, which requires careful handling. The shear strength test data from this method can show considerable scatter which has been attributed to certain "uncontrollable" factors in the test procedure [5]. Recently, Dharani *et al.* [6] showed the dependence of interfacial shear stresses on the support conditions of the matrix button, in a single-fibre pull-out test. Such uncertainties can also contribute to the scatter of the test data.

In structural composites, a large number of fibres are uniformly distributed in the matrix. To simulate the fibre/matrix interface of many composite systems, it seems appropriate to work with fibre bundle or tows, rather than using individual fibres. A bundle of thin fibres is usually easier to handle. To date only a few studies have been reported on the interface between fibre bundles and matrix. Some studies on single-strand pull-out have been performed by Mai and Castino [7] on the Kevlar/epoxy system, using the same specimen geometry as in a single-fibre pull-out test with the replacement of the single fibre by the single strand. Their measurement of the interfacial shear strength was much lower than that reported by others. Mercx and Lemstra [8] studied the effect of surface treatment on Twaron D1000 aramid fibres with respect to epoxy matrix. They used the bundle pull-out method to determine the interfacial shear strength. The bundles were twisted before embedding, probably to obtain a cylindrical interfacial surface. Wells and Beaumont [9] worked on three-point bend specimens, composed of an epoxy beam with a single layer of fibre tows on the tensile side. The pull-out lengths were found to vary over the beam width, which complicated the determination of the mean pull-out length.

The test specimen that has been developed as part of this research is basically of the tensile type. It consists of two blocks of matrices, connected through a layer of fibres. Under tensile loading, the load transfer across the two matrix blocks occurs, through

* Author to whom all correspondence should be addressed.

0022–2461

the fibre layer/matrix interface. As-received Kevlar-29 fibre tows, supplied by duPont (Wilmington, DE) have been used in conjunction with a phenolic matrix. Although, it appears unconventional to use a phenolic matrix instead of an epoxy, this type of system has important applications in short-fibre frictional composites [10]. The phenolic matrix (NC 126) is a cashew-modified phenol-formaldehyde resin, supplied by the Cardolite Corporation, (Newark, NJ) and used as-received.

2. Development of the test specimen

The philosophy behind the design of the specimen has been to maintain the natural state of the fibre bundle, to be able to emulate a real composite in terms of fabrication and testing using conventional equipment. The Kevlar fibre bundle (tow) has a natural tendency to be flat unless it is twisted. This feature has been used in this experimental design. The interface, with this geometry, exists between a layer of unidirectional fibres and the adjoining bulk matrix. Macroscopically, the geometry of the interface is a plane and the test specimens could be designed based on a double-notched simple coupon specimen. The basic geometry of the specimen was a layer of fibre connecting two blocks of matrix material, as shown in Fig. 1.

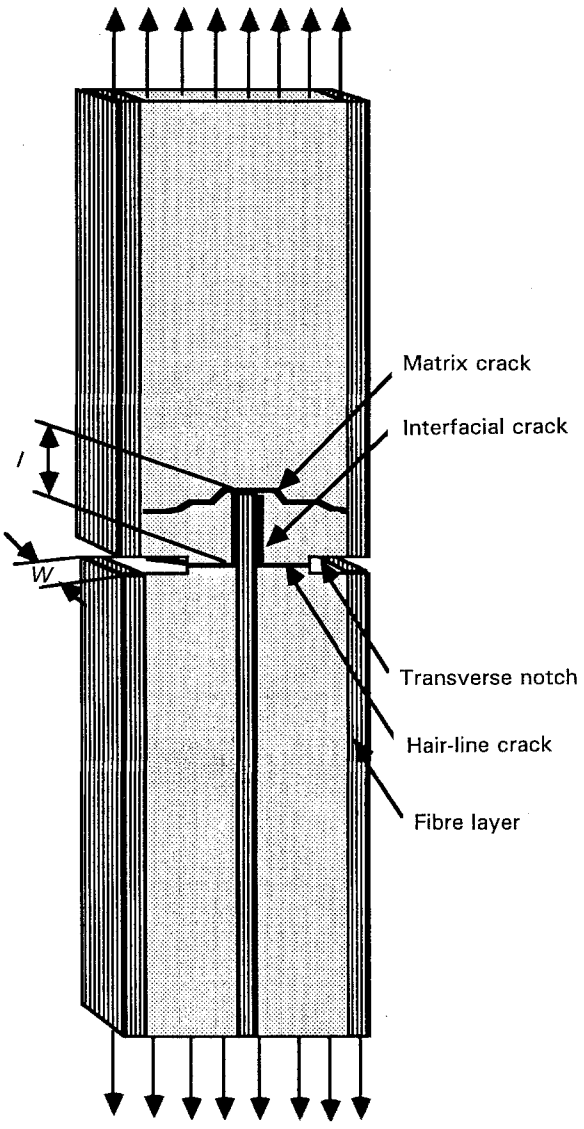

Figure 1 Bundle-debond test specimen configuration.

The specimen fabrication essentially involves the embedding of a fibre layer in the resin. The first components fabricated were the Kevlar/phenolic prepregs that could be used in the specimens. Continuous spun Kevlar fibre bundles were wound on a mandrel of a filament winding machine. A flat single layer of fibres was thus obtained. The prepregs were formed by applying the phenolic polymer on the surface of the wound fibres. Because the phenolic polymer was in dry powder form, it could not be applied directly on to the fibre, to form prepregs. Therefore, the dry polymer resin was mixed with methanol to form a thick, sticky slurry that could be applied to the fibres. The prepregs were allowed to dry in ambient conditions under flowing air. In about 2–3 days, the prepregs were dry and tac-free. However, the prepregs were dried for 10 days or more to allow for the complete removal of the dissolved methanol. The effect of the methanol present in the slurry during the drying process, on the as-received fibre coating and consequently on the fibre matrix interface was not considered in the evaluation of the test results.

The fibre prepreg was embedded in the matrix by stacking a compacted biscuit of the resin on either side of the prepreg and then curing it. Two additional layers were used on the top and bottom of the fibre-resin sandwich. The reason for using the additional fibre layers is made clear at the end of this section. The resin-biscuits were made by compacting the powder at a pressure of 21 MPa and a temperature of 60 °C. The compaction pressure was maintained for about 4–5 min, after which the pressure dropped to about 14 MPa, indicating a reduction in the void content of the biscuit. These biscuits were a crucial step in the process to obtain good quality specimens, where the fibres run straight without any twists and undulations. The biscuits were used to keep the concentration of matrix the same at all cross-sections in the mould, on either side of the central fibre layer. Thus, during the curing stage, resin flow can be reduced, on both sides of the layer of fibre. Excessive flow of resin can distort the position of the central fibre layer. The curing of the resin was done at a temperature of 160 °C and a pressure of 10.5 MPa. The pressure was applied during the final step of the curing process. Observation was made for qualitative changes in the state (amount of hardening) of the resin that leaked from the mould. Only when the resin showed signs of hardening, was the pressure applied to the mould. This procedure was necessary to prevent excessive leakage of the resin from the mould.

During the cure cycle, the temperature was maintained at 160 °C for about 5 min, followed by the cooling cycle. However, the pressure on the mould was maintained until the room temperature was attained. If the pressure was reduced during cooling, voids and cracks formed, probably due to the escaping gases and the difference in the thermal expansion coefficients of the fibre and polymer. If pressure is not

maintained until cooling occurs, the polymer will shrink away from the voids, thus enlarging them. When the mould pressure is maintained, the gases find escape routes and at the same time the polymer becomes deformed and closes any voids, as it cools. Although a pressure of 10.5 MPa was applied at the curing temperature, the pressure reading after complete cooling was about 7 MPa.

The cured plate had a dimensions of 175 mm × 51 mm. Approximately, ten specimens were cut from this plate. The width of the specimen ranged between 5 and 8 mm, while the length was about 80 mm. The edges of the specimens were ground on a belt grinder to obtain an even surface. Finally, two starter notches were cut on each specimen on either side, approximately at the middle of the specimens, Fig. 1. The starter notches had a gap of 0.38 mm, and depth approximately one quarter the thickness of the specimen. After cutting the two starter notches, the specimens were bent very lightly by hand, so that the starter notches would propagate until they reached the fibre layer. Thus the two notches break the specimen into two halves, which are connected only through a part of the central fibre layer. The length of embedment can be controlled by cutting the notch at the appropriate distance from the fibre layer end. A simple tension-type test was done on this specimen to accomplish the interface shear failure as in a single fibre pull-out test.

Interfacial failure of the central fibre layer was obtained by preventing possible matrix cracks due to the incorporation of the outer fibre layers in the specimen. The tensile stresses are shared between the two outer fibre layers, in addition to the matrix, in the "embedded piece" of the specimen. In the "tail piece" there are three fibre layers to share the tensile load in addition to the matrix itself. This configuration results in a shear-lag specimen where the transfer of load across the two pieces of the specimen occurs by

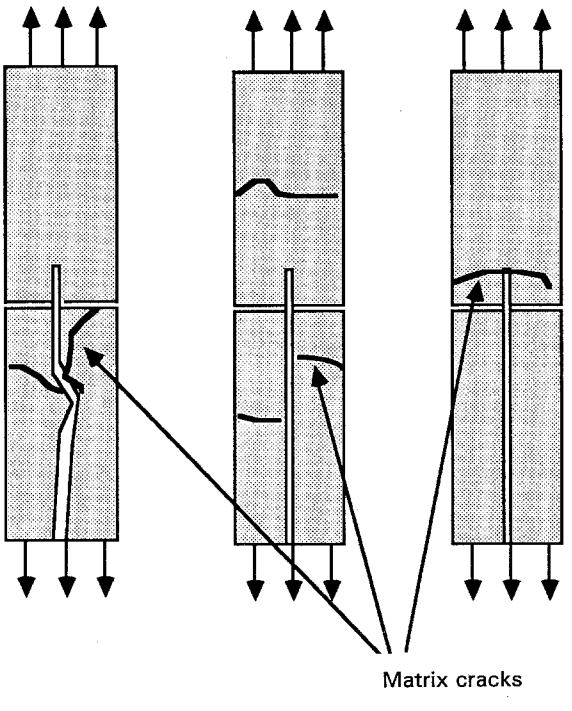

Figure 2 Matrix failure in the preliminary test specimen.

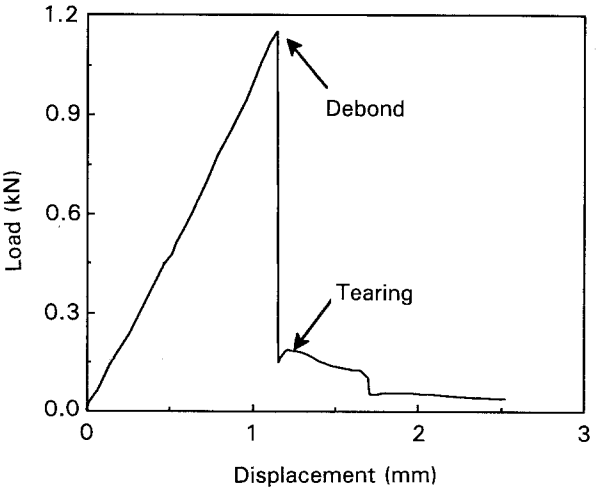

Figure 3 Typical load–displacement characteristics.

means of shear stresses that are developed at the interface of the embedded fibres and matrix. The outer fibre layers avert any possible tensile matrix failures. Initial testing of the specimens without the outer fibre layers resulted in matrix cracks as shown in Fig. 2.

All the testing was conducted on a MTS 810 system, equipped with a programmable microprofiler and computer data acquisition system. The loading rate was maintained at 0.5 mm min^{-1}. A typical load–displacement curve (Fig. 3) was composed of a linear portion starting from the origin and ending at the point of maximum load measured during the test. Once the maximum load was attained, there was a sudden drop in load to about 10%–20% of the maximum load. Further reduction in load occurred gradually with considerable displacement.

3. Theory

The shear stress distribution for a partially embedded fibre was given by Greszczuk [11], which leads to the following relation between the average shear stress and maximum shear stress

$$\tau_{av} = \tau_{max} \tanh(\alpha l)/\alpha l \quad (1)$$

where τ_{av} is the average shear stress, τ_{max} is the maximum shear stress, l is the embedded fibre length and α is a material parameter. In the above equation, when l approaches zero, the limiting value of the average shear stress is the maximum shear stress. The debond load per unit width, P_d ($= 2l\,\tau_{av}$) can be calculated as

$$P_d = P_{max} \tanh(\alpha l) \quad (2)$$

where P_{max} ($= 2\tau_{max}/\alpha$) represents a characteristic maximum load per unit width for the fibre/matrix system. In Equation 2, when the quantity αl reaches a value greater than 3, then $\tanh(\alpha l)$ is equal to 1 for all practical purposes. Hence, the debond load will be equal to the characteristic constant, P_{max}, which is independent of the embedded length and is a property of the material system. Higher values of P_{max} denotes stronger interfacial bond strength. Because α is a material system constant, adjusting the embedded fibre length so that αl would be greater than 3, would

greatly simplify the experimental evaluation of P_{max}. Equation 2 is non-linear, with two constants. An approximate value of P_{max} can be fixed based on the trend shown by the experimental P_d data with respect to embedded length. Equation 1 can be rewritten incorporating the value of P_{max} and eliminating τ_{max} to yield

$$\tau_{av} = P_{max} \tanh(\alpha l)/2l \quad (3)$$

Based on the trend shown by the experimental τ_{av} with respect to l, the value of α can be fixed approximately by using Equation 3. Further refinements of these constants can be done by variations from the approximate values and by keeping the standard deviation of the data points within acceptable limits.

4. Results and discussion

A typical experimental load–displacement curve is shown in Fig. 3. The maximum load corresponds to the bundle debond load. This is the load at which the adhesion between the fibre bundle and matrix fails. The debond does not necessarily mean that the connection between the two pieces of the specimen is completely broken. There were often fibres at the bundle/matrix interface away from the transverse crack, which were still partially attached to the matrix. The bundle, as a whole, was not effectively connected to the matrix. Any further loading was taken up by those fibres on the periphery of the bundle and the bulk of the bundle was stress free. On examination of the specimen, two cracks were found traversing along the embedment as shown in Fig. 4 and the matrix near the fibre end was completely broken. However, these broken matrix blocks were still held in place due to the outer fibre layers. At embedded lengths below 2.5 mm, often matrix cracks formed at the tip of the fibre embedment, without interfacial failure. This is probably due to stress concentration at the tip of the fibre layer at small embedded lengths. When interfacial debond occurred, loading the specimen beyond the debond, resulted in peeling of the debonded matrix blocks from the fibre bundle and also fibre tearing. The specimen started to take more load during the initial stages of the peeling process. Once the interfacial cracks were sufficiently open, the peripheral bundle fibres which are connected to the matrix blocks begin to break, resulting in a steady decline in load. The second smaller peak in the load–displacement curve corresponds to the initiation of fibre tearing. It appears that this test method would not be able to provide any information on the frictional shear strength.

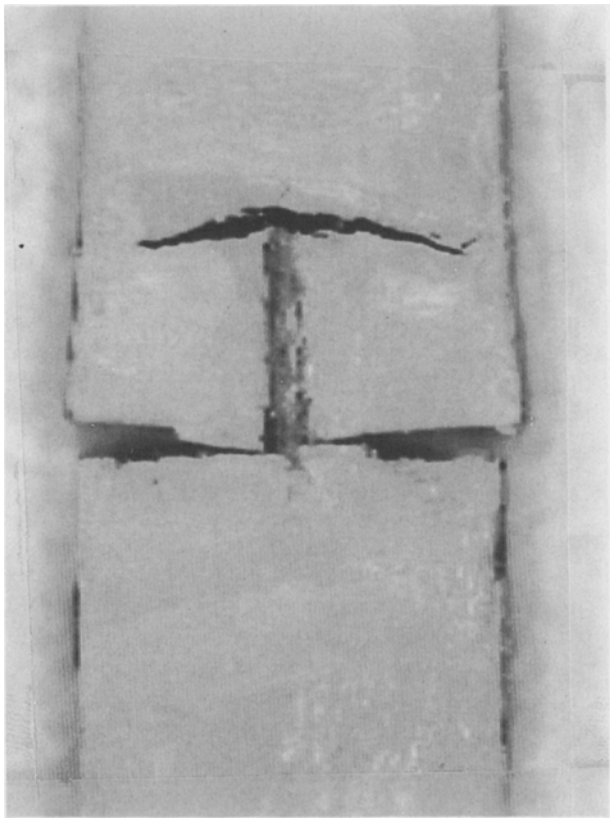

Figure 4 Typical fibre bundle/matrix interfacial shear failure.

Examination of the debonded bundle, showed very little penetration of the matrix into the bundle during the fabrication stage. This is because the phenolic resin used here is a solid and therefore has less chance of penetrating the fibre bundle. On the periphery of the bundle, not all fibres have the same degree of attachment to the matrix blocks and amongst themselves. There are some fibres which probably had a greater area of adhesion compared to some others. When the bundle interface fails, there are some fibres which are still attached to the matrix blocks. The term "bundle interface" is used here with the understanding that it is the effective connection between the fibre bundle and the matrix blocks, so that a significant stress transfer can occur between them.

After the experiments were conducted, some selected specimens were observed under the optical microscope. The fracture surface of the matrix blocks debonded from the fibre bundle, contained some of the peeled fibres partly adhering and partly free. The surface was rough due to the imprints of the fibre. At short embedded lengths, the fracture surface of the matrix had very few fibres on it. The specimens with longer embedded lengths, showed more fibres on the matrix fracture surface. This can be attributed to the larger shear stress gradient at the interface which is not very effective in debonding all along the embedment. Thus there are more fibres bridging the matrix and the bundle, which undergo extensive tearing. At short embedded lengths, on the other hand, the interfacial shear stress gradients are smaller which, in turn, gives rise to nearly complete debonding and little fibre bridging and consequently less tearing.

After the debond, the embedded length for every specimen, was found as the average of up to four measurements, made using an optical comparator. The width of the embedment was obtained by measuring the width of the specimen. As a first approximation, the interfacial geometry was assumed to be planar. Hence, the average shear stress was calculated as

$$\tau_{av} = F_d/2lw \quad (4)$$

where F_d is the experimental debond load and w is the measured width. The debond load per unit width, P_d, was obtained by dividing F_d by the specimen width. The experimental values of P_d and τ_{av} were plotted with respect to the embedded length. Assuming that the shear-lag theory of Greszczuk [11] to be valid for the bundle-debond specimen, the experimental data was curve-fitted based on the method described before (Equations 2 and 3). The value of P_{max} was found to be 205 kN m^{-1}, and by setting constant α equal to 230 m^{-1} the interfacial shear strength, τ_{max}, was found to be 23.5 MPa. This value corresponds to the shear strength at zero embedded length. The assumption of a flat interfacial plane simplified the calculation of the interfacial shear strength. However, this simplification underestimated the interfacial area by neglecting the actual contour of the fracture surface. Observation of the matrix fracture surface showed the presence of a rough surface with peaks and valleys. It was not possible to measure the actual interfacial area of each specimen. However, an approximation was made wherein a row of closely packed fibres was assumed to be present at the interface. The number of fibres, n, in the row was calculated by dividing the specimen width by the nominal fibre diameter ($d = 12$ μm). The new average shear stress can then be written as

$$\tau_{av} = F_d/2n\pi rl \quad (5)$$

where r is the nominal single-fibre radius. Eliminating n in Equation 5, the average shear stress was calculated as

$$\tau_{av} = F_d/\pi wl \quad (6)$$

The debond load per unit interfacial width was computed as

$$P_d = 2F_d/\pi w \quad (7)$$

The curve fit and the experimental values of P_d and τ_{av} with respect to the embedded length are shown in Figs 5 and 6, respectively. The new value of the interfacial shear strength, τ_{max}, was found to be

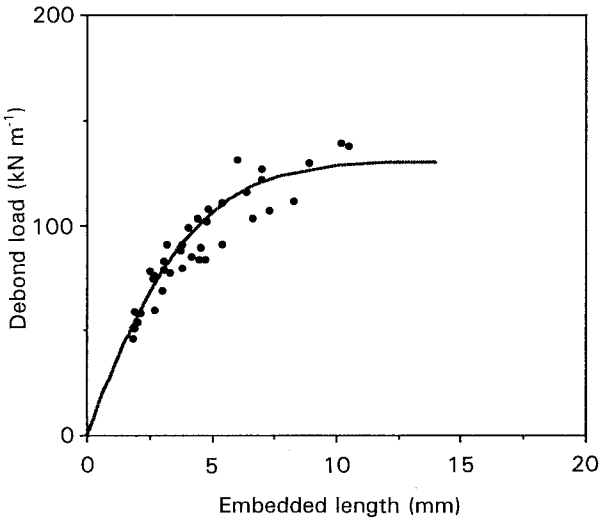

Figure 5 Variation of experimental debond load with embedded length. (——) Curve fit, (●) test data. $\alpha = 230\ m^{-1}$, $P_{max} = 130\ kN\ m^{-1}$.

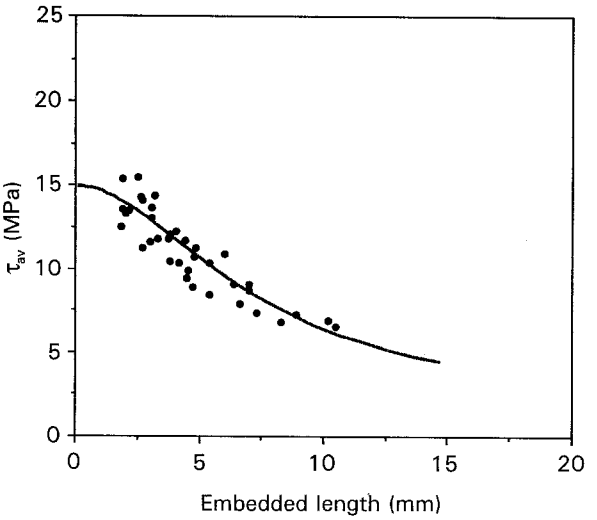

Figure 6 Variation of experimental average shear stress with embedded length. (——) Curve fit, (●) test data. $\alpha = 230\ m^{-1}$, $P_{max} = 130\ kN\ m^{-1}$.

15 MPa and P_{max} was 130 kN m^{-1}. This was a reduction of 36% in the interfacial parameters compared with those corresponding to the flat interface. There is no change in the value of α, because it does not depend on the interfacial area. The assumption of a perfectly closed pack fibre row at the interface is idealistic. The new value of the interfacial shear strength can be viewed as a conservative estimate. The first approximation of a flat interface is not realistic and does not agree with the actual fracture surface appearance. The second approximation of a closed pack fibre row is acceptable, because it better represents the fracture surface. Therefore, it is concluded that the interfacial shear strength of 15 MPa is the valid result of this test method, for Kevlar/phenolic resin composite.

A comparison of our results with those of other workers in relation to the present research is given in Table I. The only other work on Kevlar/phenolic resin interfaces is that of Subramaniam *et al.* [12]. By conducting pull-out tests, Subramaniam *et al.* determined the interfacial shear strength to be 11.2 MPa. Their value of the interfacial shear strength is ~25% lower than that of the present value. It is possible that the differences in the experimental techniques may have contributed to the differences in the strength values. It also appears that both techniques suffer from the inability to measure accurately the interfacial area. In spite of the differences in the results, the range in which the strength values fall, is reasonably good.

The present value of the interfacial shear strength of Kevlar/phenolic compares reasonably well with that of Kevlar/epoxy as seen in Table I. However, the interfacial shear strength (= 1.4 MPa) of Mai and Castino [7] for estapol-coated Kevlar/epoxy is very low in comparison with all other values. This is probably due to their overestimate of the interfacial surface area. They appear to have assumed that all the fibres in the strand ($n = 267$) contribute to the interfacial area, which seems unlikely. A most likely value of the interfacial shear strength can be determined by calculating the interfacial area, based on the strand diameter. The interfacial shear strength was recalculated

TABLE I Interfacial shear strength of aramid fibre/polymer

Reference	Matrix	Aramid fibre	Specimen type	Interfacial shear strength (MPa)
Eagles *et al.* [13]	Ionomer Polycarbonate Poly(methymethacrylate)	Sized Kevlar-49	Single-fibre pull-out	9.26 38.7 53.9
Miller *et al.* [5]	Epoxy (Epon-828)	Kevlar-49	Microbond single fibre pull-out	38
Kalantar and Drzal [14]	Epoxy (DER331)	Ethanol washed Kevlar-49	Dogbone	17[a]
Mai and Castino [7]	Epoxy	Estapol-coated Kevlar	Single-strand pull-out	1.4[a] 16[b]
Mercx and Lemstra [8]	Epoxy	Dichlomethane washed Twaron-D1000	Bundle pull-out	28.3
Subramaniam *et al.* [12]	Phenolic	As-received Kevlar-29	Bundle pull-out	11.2
Present work	Phenolic	As-received Kevlar-29	Bundle-debond	15

[a] Data read from graph.
[b] Recalculated (see text).

by us, taking the strand diameter to be 0.28 mm (from a duPont brochure) for an assumed fibre packing factor of 70%. The nominal diameter of the fibre was taken as 12 μm. The interfacial shear strength was recalculated as 16 MPa. This value is reasonable in comparison with the other values. The present interfacial shear strength of Kevlar/phenolic resin is lower than that of Kevlar/epoxy [5, 8]. This trend is also appropriate, because Kevlar is not expected to bond as well to phenolics as to epoxies.

Examination of the experimental debond load data obtained from the bundle-debond specimens showed that the scatter was not high (~10% standard deviation). However, in the microbond test, scatter of data is normally high. Miller *et al.* [5], reasoned that the variation of chemical, physical or morphological characteristics along the length of the fibre, leads to the scatter of bond strength in the microbond test. In the bundle-debond specimen, the effect of the variations of the fibre surface characteristics will be averaged, because fibre bundles are used. Consequently, any scatter of data in the bundle-debond test, will be due to fabrication and testing conditions which can be controlled within certain limits.

5. Conclusions

A simple and effective method, called bundle-debonding, has been developed for the characterization of interfacial shear strength of fibre bundles and matrix. Satisfactory interfacial debonding was obtained for Kevlar-29 embedment in phenolic matrix, ranging between 2.5 and 8 mm. At large embedded lengths, the interfacial fracture surface of the matrix showed more fibre bridging compared to that at small embedded lengths. The interfacial debond strength of Kevlar-29/phenolic resin has been determined to be 15 MPa. However, frictional shear strength cannot be obtained by this method due to crack opening at the interface.

Acknowledgements

The authors thank E. I. du Pont de Nemours, Cardolite Corporation and the Center for Advanced Technology, University of Missouri-Rolla, for their financial support of the Friction Materials Laboratory.

References

1. H. ISHIDA and G. KUMAR (eds), "Molecular Characterization of Composite Interfaces" (Plenum Press, New York, 1985).
2. H. ISHIDA and J. L. KOENIG (eds), "Composite Interfaces" (Elsevier Science, New York, 1986).
3. F. R. JONES (ed), "Interfacial Phenomena in Composite Materials" (Butterworths, Boston, 1989).
4. J. P. FAVRE, *ibid.* p. 7.
5. B. MILLER, P. MURI and L. REBENFELD, *Compos. Sci. Technol.* **28** (1987) 17.
6. L. R. DHARANI, M. N. RAHAMAN and S.-H. WANG, *J. Mater. Sci.* **25** (1990) 655.
7. W. MAI and F. CASTINO, *J. Mater. Sci. Lett.* **4** (1985) 505.
8. F. P. M. MERCX and P. J. LEMSTRA, *Polym. Commun.* **31** (1990) 252.
9. J. K. WELLS and P. W. R. BEAUMONT, *J. Mater. Sci.* **20** (1985) 1275.
10. H. Y. LOKEN, SAE Technical Paper 800667 (1980).
11. L. B. GRESZCZUK, in "Interfaces in Composites" ASTM STP 452 (American Society for Testing and Materials, Philadelphia, PA, 1969) p. 42.
12. N. SUBRAMANIAM, F. D. BLUM, P. GOPAL and L. R. DHARANI, *SAMPE Quart.* **24** (1993) 15.
13. D. B. EAGLES, B. F. BLUMENTRITT and L. STUART, *J. Appl. Polym. Sci.* **20** (1976) 435.
14. J. KALANTAR and L. T. DRZAL, *J. Mater. Sci.* **25** (1990) 4194.

Received 22 July 1992
and accepted 31 August 1993